

VERIFICATION OF FRAME INDIFFERENCE FOR COMPLICATED NUMERICAL CONSTITUTIVE MODELS

Krishna Kamojjala*, Rebecca M. Brannon*

*Department of Mechanical Engineering,
University of Utah, 50 S. Central Campus
Dr., Salt Lake City, UT 84112.

ABSTRACT

The principle of material frame indifference requires spatial stresses to rotate with the material, whereas reference stresses must be insensitive to rotation. Testing of a classical uniaxial strain problem with superimposed rotation reveals that a very common approach to strong incremental objectivity taken in finite element codes to satisfy frame indifference (namely working in an approximate un-rotated frame) fails this simplistic test. A more complicated verification example is constructed based on the method of manufactured solutions (MMS) which involves the same character of loading at all points, providing a means to test any nonlinear-elastic arbitrarily anisotropic constitutive model.

INTRODUCTION

The principle of material frame indifference (PMFI) requires that if a deformed material is rotated, then the spatial tractions and stresses should rotate along with it whereas the reference stresses must be insensitive to the rotation. A review of material frame indifference is already presented in [1]. This concept is different from basis indifference. The difference between basis indifference and frame indifference is the initial configuration. Figure 1 represents a simple shear under basis rotation and superimposed rotation. Under basis rotation, both the initial configuration and the deformed configuration are rotated whereas under superimposed rotation, only the deformed configuration is rotated. The PMFI demands that the stress for deformation in Fig. 1.(b) should be same as Fig. 1.(a) except rotated appropriately. PMFI does not guarantee the accuracy of the material model. It is one of the physical principles tested to check material models for consistency under superimposed rotations and translations.

Verification & Validation of development codes with complicated numerical constitutive models is important for testing the accuracy and robustness of these methods [3]. Verification is a process that is used to evaluate the correctness of the solution of the governing equations in the code. Validation is a quality control process of establishing evidence that the equations themselves provide an acceptable description of reality with respect to intended requirements,

and is done by comparing with the experimental data. The MMS is an accepted standard of verification testing in the scientific community that has been used extensively in fluid mechanics [4], but is rarely demonstrated in solid mechanics because of the increased mathematical complexity. MMS is a process of determining the external body force required to achieve a pre-decided deformation analytically. Then the code is verified by running it with the computed body force and demonstrating that the pre-decided deformation is achieved.

This paper will first focus on PMFI where a uniaxial strain problem with superimposed rotation is tested with and without a frame indifferent constitutive model. An analytical solution for the simplest possible constitutive model (linear elasticity) is sufficient to demonstrate that a common approximation used in implementations of strong incremental objectivity [6] results in failure to satisfy the PMFI. Subsequently a MMS approach will be used to construct a more complicated verification example of large deformation and large rotation of a thick vertical beam that will serve as a means to test arbitrarily nonlinear anisotropic elastic constitutive model for simultaneous basis and frame indifference.

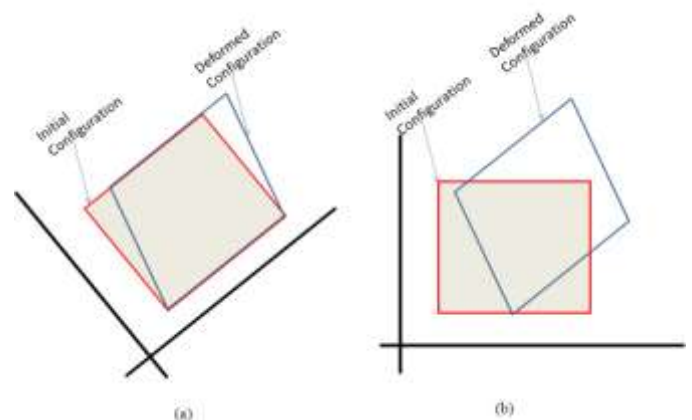


Figure 1: (a) Basis rotation (b) Superimposed rotation.

NOMENCLATURE

σ_n	Cauchy stress at time step n
\mathbf{D}_n	Symmetric part of the velocity gradient at time step n
\mathbf{R}_n	Rotation matrix at time step n
\mathbf{b}	Body force vector
\mathbf{a}	Acceleration vector
ρ	Material density
λ	Stretch
λ^*	Lame modulus
μ	Shear modulus

SINGLE ELEMENT TEST

The concept of frame indifference is illustrated using a classical single element test [7]. The test problem is described as follows:

- The element undergoes uniaxial strain (along the x-axis) from time $t=0$ to $t=1$.
- This deformed configuration undergoes superimposed rotation of 90 degrees (about the z-axis) from time $t=1$ to $t=2$.

The exact solution during the second leg is given by:

$$\boldsymbol{\sigma} = \mathbf{R} \cdot \bar{\boldsymbol{\sigma}} \cdot \mathbf{R}^T \quad (1)$$

where

$$\mathbf{R} = \begin{pmatrix} \cos[\theta] & -\sin[\theta] & 0 \\ \sin[\theta] & \cos[\theta] & 0 \\ 0 & 0 & 1 \end{pmatrix},$$

$$\bar{\boldsymbol{\sigma}} = \begin{pmatrix} \sigma_A & 0 & 0 \\ 0 & \sigma_L & 0 \\ 0 & 0 & \sigma_L \end{pmatrix},$$

$\bar{\boldsymbol{\sigma}}$ is the un-rotated stress, σ_A is the axial stress and σ_L is the lateral stress.

Thus

$$\boldsymbol{\sigma} = \begin{pmatrix} \sigma_A \cos^2[\theta] + \sigma_L \sin^2[\theta] & (\sigma_A - \sigma_L) \sin[\theta] \cos[\theta] & 0 \\ (\sigma_A - \sigma_L) \sin[\theta] \cos[\theta] & \sigma_L \cos^2[\theta] + \sigma_A \sin^2[\theta] & 0 \\ 0 & 0 & \sigma_L \end{pmatrix}$$

Figure 2. shows the plots of normalized stress components vs. time for the above mentioned analytical solution. This shows that, although the principal stresses do not change during rotation, the stress components must vary to account for rotation of the principal directions of stress.

The Uintah computational framework [8] at the University of Utah was used for all the numerical simulations shown in this paper. The hypoelastic constitutive model in the Uintah framework was chosen to run the test problem. The Cauchy

stress $\boldsymbol{\sigma}$ is governed by some function of the symmetric part of the velocity gradient \mathbf{D} . This can be represented as:

$$\boldsymbol{\sigma}_{n+1} = \boldsymbol{\sigma}_n + g(\mathbf{D}_n) \quad (2)$$

Since this formulation includes no objective rates or Lie transformations to an un-rotated configuration, it is well known to violate frame indifference. Figure 3. shows the model prediction for the stress (normalized by 1.06 times the peak stress) vs. time. During the first time interval when the

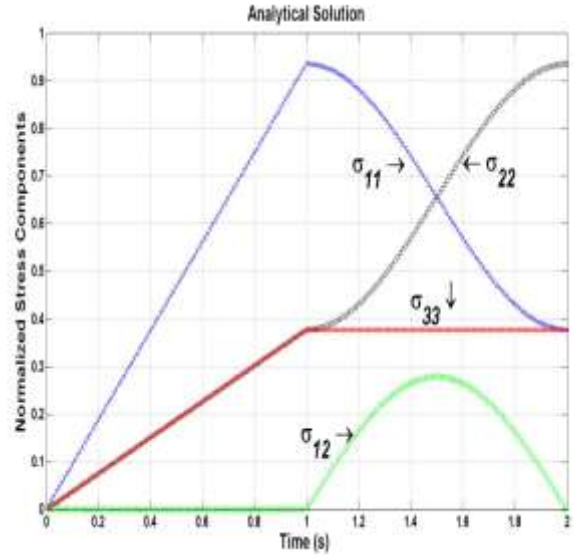


Figure 2: Normalized stress components vs. time for the analytical solution

element undergoes uniaxial strain, the plot shows correct linear response of the 11, 22 and 33 components of stresses with the shear component being zero. During the second time interval, however, when the deformed element undergoes superimposed rotation, the symmetric part of the velocity gradient is zero. Hence the values of all the stress components remain constant and equal to that of the value at the end of the first time interval. This reveals that this constitutive model is not self consistent under superimposed rotations and therefore fails the frame indifference test.

To satisfy frame indifference, several constitutive models in the Uintah framework used an approximated un-rotated frame. A flawed schema, summarized in Fig. 4., had been as follows:

- Stress and symmetric part of the velocity gradient are initialized at the beginning of the step.
- The stress and symmetric part of the velocity gradient needed as input to the constitutive model were un-rotated using the polar rotation *at the end* of the step.
- The updated stress coming out of the constitutive model was re-rotated using *the same* rotation (*i.e.*, at the end of the step).

The test problem was run on one of the constitutive models in Uintah that requires the host code to apply the model in an un-rotated frame to satisfy frame indifference.

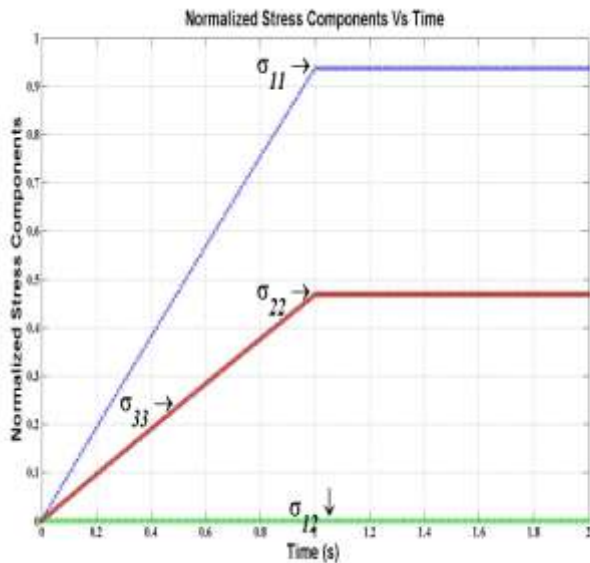


Figure 3: Normalized stress components vs. time for hypoelastic constitutive model

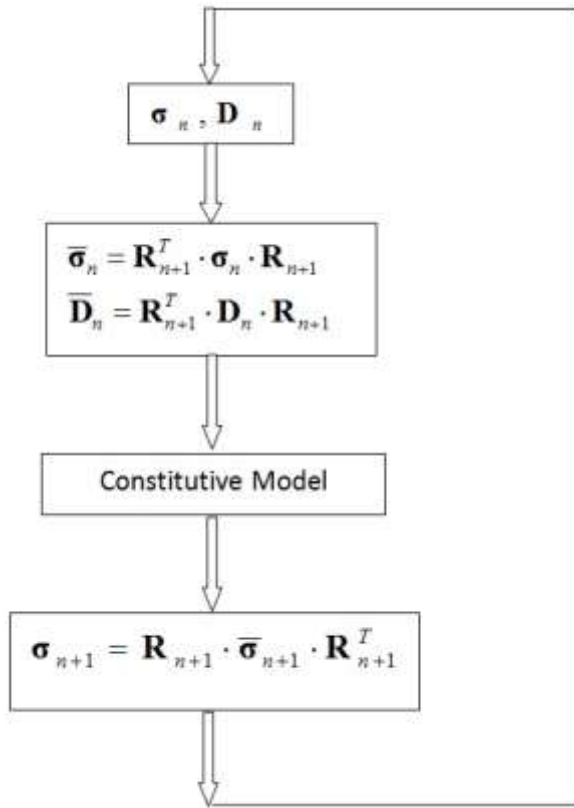


Figure 4: Flawed stress update algorithm

Figure 5. shows the normalized stress components vs. time plot for this model when the flawed schema of Fig. 4 was used in the host code. The results reveal that the constitutive model failed this simplistic test for frame indifference. The model behaves as expected for the first time interval when the element is under uniaxial strain. During the second time interval, since the symmetric part of the velocity gradient is

zero, the constitutive model correctly predicted that the *un-rotated* stress remained unchanged. Therefore, the values of $\bar{\sigma}_n$ and $\bar{\sigma}_{n+1}$ are equal. Since the stress is un-rotated by \mathbf{R}_{n+1} before sending it to the constitutive model and then re-rotated by the same amount after coming out of the constitutive model, the value of spatial Cauchy stress σ_{n+1} does not change as it should during this interval.

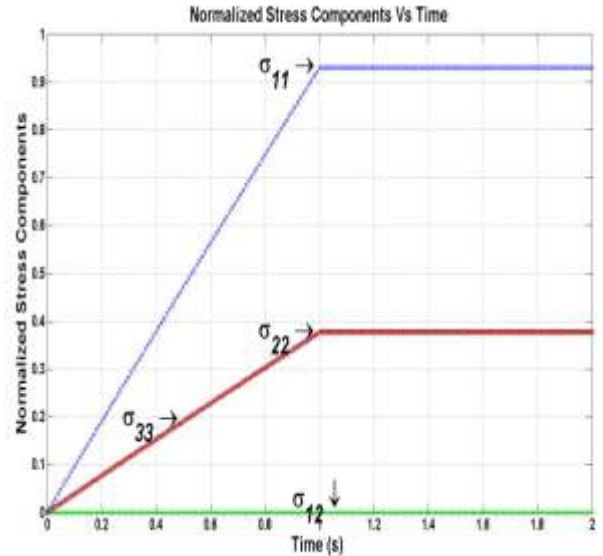


Figure 5: Normalized stress components vs. time for the constitutive model that uses the un-rotation schema as in Fig. 4.

Hence the values of all the stress components remain constant and equal to that of the value at the end of the first time interval. Reducing the time step to a very small value will not solve the problem because of the use of the same rotation tensor for both operations, which implies an erroneously constant stress regardless of the time step. To rectify this problem, the following changes were made to the un-rotation schema

- The stress and symmetric part of the velocity gradient are un-rotated using \mathbf{R}_n .
- The stress output from the constitutive model is re-rotated using \mathbf{R}_{n+1} .

Figure 6. shows that this corrected incremental strong objectivity algorithm satisfies the principle of material frame indifference because the stresses now correctly rotates with the deformed material. The following observations can be made from Fig. 6.:

- At the end of the second time interval, the value of σ_{11} is equal to the value of σ_{22} at the end of the first time interval.
- At the end of the second time interval, the value of σ_{22} is equal to the value of σ_{11} at the end of the first time interval.
- During the second time interval, the value of σ_{33} is zero because it's the out of plane stress. Hence, the

value of σ_{33} remains constant and is equal to that of the value at the end of the first time interval.

- During the second time interval, the σ_{12} has a peak value of $\frac{\sigma_{11} - \sigma_{22}}{2}$ at the half-time of the second interval.

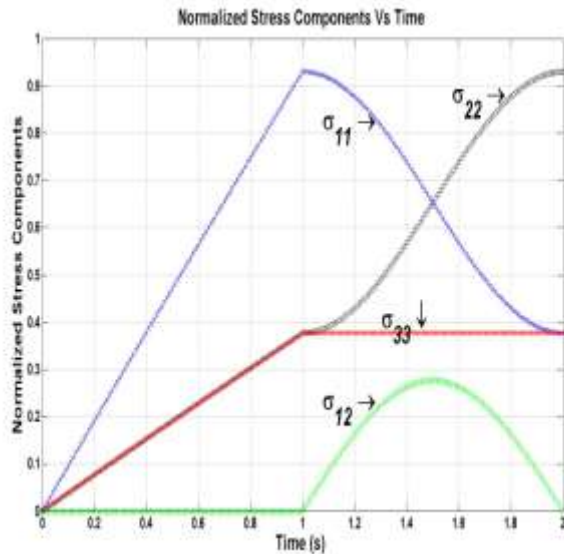


Figure 6: Normalized stress components vs. time for the constitutive model that uses the changed un-rotation scheme

Therefore, this test reveals that, for the problems involving large material rotation, different polar rotation tensors need to be used. Penetration simulations, for example, involve large material deformations and rotations. A penetration simulation was run in Uintah with and without the change to the stress un-rotation and was compared. Figure 7. shows that normalized penetration depth vs. time was not significantly improved by the frame indifference bug correction, but work is underway to assess the influence of the changes on material response, such as damage along the penetration channel, that is expected to be more sensitive to frame indifference errors.

METHOD OF MANUFACTURED SOLUTIONS

The Method of manufactured solutions is a systematic process of verifying the development codes by running them with the analytically computed external body force and demonstrating the pre-decided deformation. A simple 1-D example for MMS is already available [9] which is constructed based on [10]. This method had been successfully used for verification testing in the scientific community including fluid heat transfer [12], fluid-structure interactions [13] and extensively in fluid mechanics. This section will focus on analytically determining the external body force required for large deformation and large rotation of a thick vertical beam using this technique. This problem will have the same character of loading at all instants of time as described in the single element section. At all points, the body will undergo a uniaxial strain under superimposed rotation. Figure 8. shows the snapshot of the deformation of bending beam in time.

The motion is governed by the equation:

$$\nabla \cdot \boldsymbol{\sigma} + \rho \mathbf{b} = \rho \mathbf{a} \quad (3)$$

where \mathbf{a} is the acceleration and \mathbf{b} is the body force. In the MMS, the deformation is pre-decided so that acceleration is known. Moreover, for an elastic material model, the stress is a known function of deformation, which allows the stress

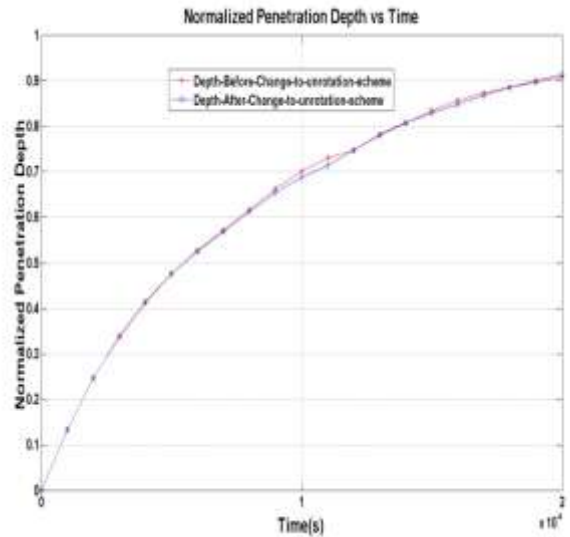


Figure 7: Normalized penetration depth vs. time comparison

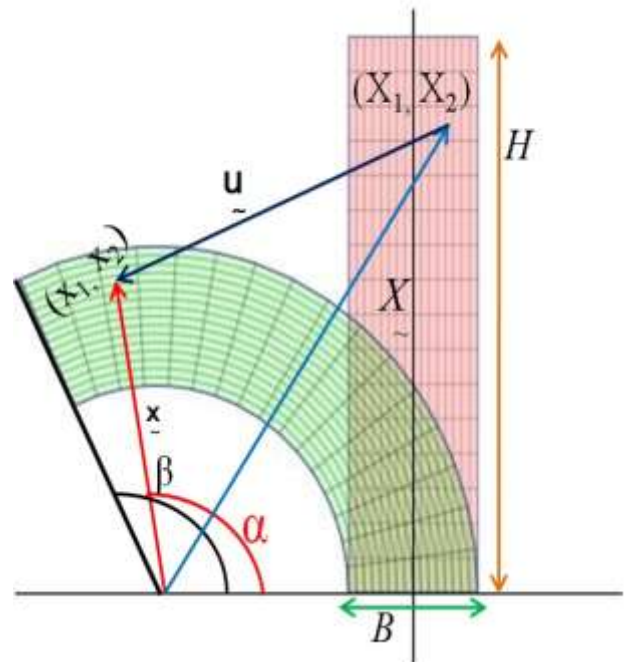


Figure 8: Snapshot of the deformation in time.

divergence to be considered as known. Therefore, the goal is to find these functions and substitute the results into Eq. (3) to find the body force (which, in the MMS, then is used as the forcing function in the code to see if the prediction recovers the pre-decided deformation). Indicinal notation for the body force \mathbf{b} in the above equation is given by

$$b_i = a_i - \frac{f_i}{\rho} \quad (4)$$

where f_i is the i^{th} component of divergence of the Cauchy stress. The bending of the beam of height H and base B is parameterized by a time-varying parameter $\beta[t]$ equal to the angle of the top surface of the beam. The corresponding mapping from an initial position \mathbf{X} to deformed position \mathbf{x} is

$$\begin{cases} x_1 \\ x_2 \end{cases} = \begin{cases} \frac{-H}{\beta} + \left(\frac{H}{\beta} + X_1\right) \cos\left(\frac{\beta X_2}{H}\right) \\ \left(\frac{H}{\beta} + X_1\right) \sin\left(\frac{\beta X_2}{H}\right) \end{cases} \quad (5)$$

As can be confirmed by direct substitution, the deformation gradient decomposed into rotation and stretch $\mathbf{F} = \mathbf{R} \cdot \mathbf{U}$, is computed by the following sequence of calculations where α is the angle of rotation at the material point of interest, λ is the amount of stretch in the 2-direction, \mathbf{R} is the rotation tensor and \mathbf{U} is the stretch tensor.

$$\alpha = \frac{\beta[t]X_2}{H}, \lambda = \frac{\beta[t]X_1}{H} + 1,$$

$$\mathbf{R} = \begin{pmatrix} \cos[\alpha] & -\sin[\alpha] & 0 \\ \sin[\alpha] & \cos[\alpha] & 0 \\ 0 & 0 & 1 \end{pmatrix}, \quad (6)$$

$$\mathbf{U} = \begin{pmatrix} 1 & 0 & 0 \\ 0 & \lambda & 0 \\ 0 & 0 & 1 \end{pmatrix}$$

The following section will derive the contribution of the force from the material acceleration and from the stress divergence. Then these values can be substituted in Eq. (4) to evaluate the body forces.

Force contribution from the divergence of the stress.

In the MMS, we assume that we have all the information in Eq. (3) except the body force. It is possible (e.g. by running a single-element model driver) to obtain all stress components as a function of uniaxial stain stretching in the 2-direction WITHOUT ROTATION. Suppose, for example, the constitutive model is the following simple NeoHookean model:

$$\boldsymbol{\sigma} = \frac{\lambda^* \text{Log}[J]}{J} \mathbf{I} + \frac{\mu}{J} [\mathbf{F} \cdot \mathbf{F}^T - \mathbf{I}] \quad (7)$$

where λ^* is the Lamé modulus, μ is the shear modulus, J is the Jacobian, \mathbf{F} is the deformation gradient and \mathbf{I} is the identity tensor. We have chosen λ^* to be Lamé modulus because λ is already defined to be the amount of stretch in the 2-direction. For uniaxial strain in the 2-direction, the rotation is $\mathbf{R} = \mathbf{I}$, and therefore the deformation gradient is $\mathbf{F} = \mathbf{U}$, and its Jacobian is λ :

$$\mathbf{U} = \begin{pmatrix} 1 & 0 & 0 \\ 0 & \lambda & 0 \\ 0 & 0 & 1 \end{pmatrix} \quad (8)$$

$$J = \det[\mathbf{U}] = \lambda$$

Computing the un-rotated stress for the simple NeoHookean model, because that model is an isotropic model, it has axial and lateral stress components as the only nonzero functions of uniaxial stretch λ . To apply this manufactured solution to an *arbitrary*, potentially anisotropic and even more nonlinear, elastic constitutive model, the upcoming analysis presumes only that the response functions for all components of stress under uniaxial strain in the 2-direction are known; *i.e.*,

$$\bar{\boldsymbol{\sigma}} = \begin{pmatrix} \sigma_{11}[\lambda] & \sigma_{12}[\lambda] & \sigma_{13}[\lambda] \\ \sigma_{21}[\lambda] & \sigma_{22}[\lambda] & \sigma_{23}[\lambda] \\ \sigma_{31}[\lambda] & \sigma_{32}[\lambda] & \sigma_{33}[\lambda] \end{pmatrix} \quad (9)$$

Then Cauchy stress $\boldsymbol{\sigma}$ is computed using

$$\boldsymbol{\sigma} = \mathbf{R} \cdot \bar{\boldsymbol{\sigma}} \cdot \mathbf{R}^T \quad (10)$$

where \mathbf{R} is the rotation tensor. Now we need the divergence of the Cauchy stress. Substituting Eq. (10) in the indicial form of the stress divergence gives

$$\frac{\partial \sigma_{ij}}{\partial x_j} = \frac{\partial (R_{im} \cdot \bar{\sigma}_{mn} \cdot R_{jn})}{\partial x_j} \quad (11)$$

By the product rule,

$$\begin{aligned} \frac{\partial \sigma_{ij}}{\partial x_j} &= \frac{\partial (R_{im})}{\partial x_j} \bar{\sigma}_{mn} R_{jn} + R_{im} \bar{\sigma}_{mn} \frac{\partial (R_{jn})}{\partial x_j} \\ &+ R_{im} \frac{\partial (\bar{\sigma}_{mn})}{\partial x_j} R_{jn} \end{aligned} \quad (12)$$

Recalling from Eq. (9) that $\bar{\boldsymbol{\sigma}}$ depends only on the stretch λ , while Eq. (6) shows that the polar rotation \mathbf{R} depends only on the rotation angle α , using chain rule

$$\frac{\partial (R_{im})}{\partial x_j} = \frac{d(R_{im})}{d\alpha} \frac{\partial \alpha}{\partial x_j} \quad (13)$$

and

$$\frac{\partial (\bar{\sigma}_{mn})}{\partial x_j} = \frac{d(\bar{\sigma}_{mn})}{d\lambda} \frac{\partial \lambda}{\partial x_j} \quad (14)$$

Using the expression for \mathbf{R} from Eq. (6),

$$\frac{d\mathbf{R}}{d\alpha} = \begin{pmatrix} -\sin[\alpha] & -\cos[\alpha] & 0 \\ \cos[\alpha] & -\sin[\alpha] & 0 \\ 0 & 0 & 0 \end{pmatrix} = \mathbf{A} \cdot \mathbf{R}$$

where

$$[\mathbf{A}] = \begin{pmatrix} 0 & -1 & 0 \\ 1 & 0 & 0 \\ 0 & 0 & 0 \end{pmatrix}$$

Therefore Eq. (13) becomes

$$\frac{\partial(R_{im})}{\partial x_j} = A_{ip} R_{pm} \frac{\partial \alpha}{\partial x_j} \quad (15)$$

Recalling that

$$\alpha = \frac{\beta[t]X_2}{H}$$

Note that

$$\frac{\partial \alpha}{\partial x_j} = \frac{d\alpha}{dX_s} \frac{\partial X_s}{\partial x_j} = \frac{d\alpha}{dX_s} F_{sj}^{-1} = \frac{d\alpha}{dX_s} U_{sa}^{-1} R_{ja} \quad (16)$$

Therefore Eq. (15) becomes

$$\frac{\partial(R_{im})}{\partial x_j} = A_{ip} R_{pm} \frac{d\alpha}{dX_s} U_{sa}^{-1} R_{ja} \quad (17)$$

This implies that

$$\frac{\partial(R_{jn})}{\partial x_j} = A_{jp} R_{pn} \frac{d\alpha}{dX_s} U_{sa}^{-1} R_{ja} \quad (18)$$

The expressions for gradients of rotation expressed in Eq. (17) and Eq. (18) are substituted in Eq. (12) to give

$$f_i = \frac{\partial \sigma_{ij}}{\partial x_j} = A_{ip} R_{pm} \frac{d\alpha}{dX_s} U_{sa}^{-1} R_{ja} \bar{\sigma}_{mn} R_{jn} + R_{im} \frac{\partial(\bar{\sigma}_{mn})}{\partial x_j} R_{jn} + R_{im} \bar{\sigma}_{mn} A_{jp} R_{pn} \frac{d\alpha}{dX_s} U_{sa}^{-1} R_{ja} \quad (19)$$

Multiplying both sides of the Eq. (19) using R_{iq} and simplifying using the fact that \mathbf{R} is orthogonal, we have

$$\bar{f}_q = R_{iq} f_i = A_{qm} \frac{\partial \alpha}{\partial X_s} U_{sn}^{-1} \bar{\sigma}_{mn} + \frac{\partial(\bar{\sigma}_{qn})}{\partial x_j} R_{jn} + \bar{\sigma}_{qn} A_{an} \frac{\partial \alpha}{\partial X_s} U_{sa}^{-1} \quad (20)$$

Recall that the un-rotated stress depends only on the stretch λ , and λ depends on \mathbf{X} . Therefore, by chain rule,

$$\frac{\partial(\bar{\sigma}_{qn})}{\partial x_j} = \frac{d(\bar{\sigma}_{qn})}{d\lambda} \frac{\partial \lambda}{\partial x_j} = \frac{d(\bar{\sigma}_{qn})}{d\lambda} \frac{d\lambda}{dX_p} \frac{\partial X_p}{\partial x_j} \quad (21)$$

Eq. (21) can still be reduced to

$$\frac{\partial(\bar{\sigma}_{qn})}{\partial x_j} = \frac{d(\bar{\sigma}_{qn})}{d\lambda} \frac{d\lambda}{dX_p} U_{pt}^{-1} R_{jt} \quad (22)$$

Using the definitions of λ , \mathbf{U} and \mathbf{A} and substituting Eq. (22) in Eq. (20), we have

$$\bar{f}_q = \frac{\beta}{H\lambda} \left(A_{q1} \bar{\sigma}_{12} + A_{q2} \bar{\sigma}_{22} + \lambda \frac{d\bar{\sigma}_{q1}}{d\lambda} + \bar{\sigma}_{q1} \right) \quad (23)$$

Thus, un-rotated force is

$$\begin{aligned} \bar{f}_1 &= \frac{\beta}{H\lambda} \left(-\bar{\sigma}_{22} + \lambda \frac{d\bar{\sigma}_{11}}{d\lambda} + \bar{\sigma}_{11} \right) \\ \bar{f}_2 &= \frac{\beta}{H\lambda} \left(\bar{\sigma}_{12} + \lambda \frac{d\bar{\sigma}_{21}}{d\lambda} + \bar{\sigma}_{21} \right) \\ \bar{f}_3 &= \frac{\beta}{H\lambda} \left(\lambda \frac{d\bar{\sigma}_{31}}{d\lambda} + \bar{\sigma}_{31} \right) \end{aligned} \quad (24)$$

The force contributions from the divergence of stress above apply even to anisotropic constitutive models. For the special case of an isotropic constitutive model, the un-rotated stress will be diagonal, giving

$$\begin{aligned} \bar{f}_1 &= \frac{\beta}{H\lambda} \left(-\bar{\sigma}_{22} + \lambda \frac{d\bar{\sigma}_{11}}{d\lambda} + \bar{\sigma}_{11} \right) \\ \bar{f}_2 &= 0 \\ \bar{f}_3 &= 0 \end{aligned} \quad (25)$$

These are the un-rotated force components. To apply these in a calculation of the body force for the manufactured solution, the actual force vector can be computed by recalling that $\mathbf{f} = \mathbf{R} \cdot \bar{\mathbf{f}}$. Therefore,

$$\begin{aligned} \mathbf{f} &= f_r \mathbf{e}_r \\ \text{where} \\ f_r &= \frac{\beta}{H\lambda} \left(-\bar{\sigma}_{22} + \lambda \frac{d\bar{\sigma}_{11}}{d\lambda} + \bar{\sigma}_{11} \right) \end{aligned} \quad (26)$$

and

$$\mathbf{e}_r = \cos[\alpha] \mathbf{e}_1 + \sin[\alpha] \mathbf{e}_2 \quad (27)$$

For the NeoHookean constitutive model used in this paper, the value of \mathbf{f} comes out to be

$$f_r = - \frac{\beta[t] \left(H^2 \lambda^* \left(-1 + \text{Log} \left[1 + \frac{X_1 \beta[t]}{H} \right] \right) + 2H\mu X_1 \beta[t] \right)}{H(H + X_1 \beta[t])^2} \quad (28)$$

In general, the force vector for an anisotropic elastic material will include an angular component so that,

$$\mathbf{f} = f_r \mathbf{e}_r + f_\theta \mathbf{e}_\theta \quad (29)$$

Force contribution from the material acceleration.

Determining the contribution of force from the material acceleration is relatively easy because we already have the relation between \mathbf{x} and \mathbf{X} . Acceleration is simply

$$\mathbf{a} = \left(\frac{\partial^2 \mathbf{x}}{\partial t^2} \right)_{\mathbf{x}}$$

The final result for the acceleration vector comes out to be

$$\mathbf{a} = a_r \mathbf{e}_r + a_\theta \mathbf{e}_\theta \quad (30)$$

where

$$a_r = \frac{- \left(2H^3 \left(-1 + \cos \left[\frac{X_2 \beta[t]}{H} \right] \right) + HX_2^2 \beta[t]^2 + X_1 X_2^2 \beta[t]^3 \right) \beta'[t]^2}{H^2 \beta[t]^3} \quad (31)$$

$$+ \frac{H^3 \left(-1 + \cos \left[\frac{X_2 \beta[t]}{H} \right] \right) \beta[t] \beta''[t]}{H^2 \beta[t]^3}$$

$$a_\theta = \frac{\left(2H \left(H \sin \left[\frac{X_2 \beta[t]}{H} \right] - X_2 \beta[t] \right) \right) \beta'[t]^2}{H \beta[t]^3} \quad (32)$$

$$+ \frac{\left(-H^2 \sin \left[\frac{X_2 \beta[t]}{H} \right] + HX_2 \beta[t] + X_1 X_2 \beta[t]^2 \right) \beta[t] \beta''[t]}{H \beta[t]^3}$$

$$\mathbf{e}_r = \cos[\alpha] \mathbf{e}_1 + \sin[\alpha] \mathbf{e}_2 \text{ and}$$

$$\mathbf{e}_\theta = -\sin[\alpha] \mathbf{e}_1 + \cos[\alpha] \mathbf{e}_2$$

Density is given by the following equation:

$$\rho = \rho_0 \lambda \quad (33)$$

Substituting Eqs. (28), (31), (32), and (33) into Eq. (4) gives the components of the total body force required for this deformation:

$$\mathbf{b} = b_r \mathbf{e}_r + b_\theta \mathbf{e}_\theta \quad (34)$$

where

$$b_r = a_r - \frac{f_r}{\rho},$$

$$b_\theta = a_\theta - \frac{f_\theta}{\rho}.$$

CONCLUSIONS

This paper described the concept of frame indifference starting with a classical single element test under uniaxial strain with superimposed rotation. Results for this minimal test revealed that a very common approach taken by finite element codes to satisfy frame indifference (namely working in an approximate un-rotated frame for which rotation during the increment is implicitly neglected by using only a single orthogonal tensor for all un-rotation operations during the step) fails this simplistic test. With this test it was confirmed that if a material undergoes rotation, then different polar rotations need to be used. Also a new manufactured solution was presented for a large deformation and large rotation of a bending beam. This problem tests any generally nonlinear and anisotropic elastic constitutive model simultaneously for basis

indifference and frame indifference. It represents a rare case of manufactured solution that can be applied to arbitrary constitutive models, which was possible because the problem was designed to put all material points in the same character of deformation (uniaxial strain of various intensities with superimposed rotation).

ACKNOWLEDGMENTS

We would like to acknowledge the Schlumberger technology corporation, especially Dr. Jim Guilkey, for supporting the work. We would also like to thank the members of CSM (computational solid mechanics) group at the University of Utah for their support.

REFERENCES

- [1]. Charles G. Speziale, A Review of Material Frame-Indifference in Mechanics, *Appl. Mech. Rev.* 51, 489 (1998), DOI:10.1115/1.309901.
- [2]. Liu, I-Shih. Further remarks on Euclidean objectivity and the principle of material frame-indifference. *Continuum Mechanics and Thermodynamics*, 2005 May 01.
- [3]. Thacker, B.H., The Role of Nondeterminism in Verification and Validation of Computational Solid Mechanics Models. *Reliability & Robust Design in Automotive Engineering*, SAE Int., SP-1736, No. 2003-01-1353, SAE 2003 World Congress, Detroit, MI, 3-6 March.
- [4]. Kambiz Salari and Patrick Knupp. Code Verification by Method of Manufactured Solutions, *SANDIA REPORT*, June 2000.
- [5]. Len Schwer. Method of Manufactured Solutions: Demonstrations. <http://www.usacm.org/vnvcsm/PDF/Documents/MMS-Demo-03Sep02.pdf> (August 2002)
- [6]. Rashid MM, Incremental kinematics for finite element applications, *International journal for numerical methods in engineering* 1993; 36 (23):3937-3956
- [7]. John Robinson, A single element test. *Computer Methods in Applied Mechanics and Engineering*, Volume 7, Issue 2, February 1976, Pages 191-200, ISSN 0045-7825, DOI: 10.1016/0045-7825(76)90012-8
- [8]. Jim Guilkey, Todd Harman, Justin Luitjens, John Schmidt, Jeremy Thornock, J. Davison de St. Germain, Siddharth Shankar, Joseph Peterson, Carson Brownlee. *Uintah User guide, SCI Institute Technical Report*, 2009.
- [9]. B. Banerjee, Method of manufactured solutions, www.eng.utah.edu/banerjee/Notes/MMS.pdf (October 2006).
- [10]. R. C. Batra and X. Q. Liang, Finite dynamic deformations of smart structures, *Computational Mechanics*, 20, 427-438, 1997.
- [11]. R. C. Batra and B. M. Love, Multiscale analysis of adiabatic shear bands in tungsten heavy alloy particulate composites, *International Journal for Multiscale Computational Engineering*, 4(1), 95-114. 2006.
- [12]. Brunner, T. A., Development of a grey nonlinear thermal radiation diffusion verification problem.

Transactions of the American Nuclear Society 95, 876-878. 2006.

- [13]. Tremblay, D., Etienne, S. & Pelletier, D. Code verification and the method of manufactured solutions for fluid-structure interaction problems. *In 36th AIAA Fluid Dynamics Conference*, vol. 2, pp. 882-892. San Francisco, CA. 2006